Adaptive Parametric Prototype Learning for Cross-Domain Few-Shot Classification

Marzi Heidari* **Abdullah Alchihabi*** **Qing En*** **Yuhong Guo*†**
*School of Computer Science, Carleton University, Ottawa, Canada
†Canada CIFAR AI Chair, Amii, Canada
{marziheidari@cmail., abdullahalchihabi@cmail., qingen@cunet., yuhong.guo@}carleton.ca

Abstract

Cross-domain few-shot classification induces a much more challenging problem than its in-domain counterpart due to the existence of domain shifts between the training and test tasks. In this paper, we develop a novel Adaptive Parametric Prototype Learning (APPL) method under the meta-learning convention for cross-domain few-shot classification. Different from existing prototypical few-shot methods that use the averages of support instances to calculate the class prototypes, we propose to learn class prototypes from the concatenated features of the support set in a parametric fashion and meta-learn the model by enforcing prototype-based regularization on the query set. In addition, we fine-tune the model in the target domain in a transductive manner using a weighted-moving-average self-training approach on the query instances. We conduct experiments on multiple cross-domain few-shot benchmark datasets. The empirical results demonstrate that APPL yields superior performance to many state-of-the-art cross-domain few-shot learning methods.

1 INTRODUCTION

Benefiting from the development of deep neural networks, significant advancement has been achieved on image classification with large amounts of annotated data. However, obtaining extensive annotated data is time-consuming and labour-intensive, while it is difficult to generalize trained models to new categories of data. As a solution, few-shot learning (FSL) has been proposed to classify instances from unseen classes using only a few labeled instances. FSL methods usually use a base dataset with labeled instances to train a prediction model in the training phase. The model is then fine-tuned on the prediction task of novel categories with a few labeled instances (i.e. support set), and finally evaluated on the test data (i.e. query set) from the same novel categories in the testing phase. FSL has been widely studied in the in-domain settings where the training and test tasks are from the same domain (Finn et al., 2017; Snell et al., 2017; Lee et al., 2019). However, when the training and test tasks are in different domains, it poses a cross-domain few-shot learning (CDFSL) problem, which is much more challenging than its in-domain FSL counterpart due to the domain shift problem.

Recently, several methods have made progress to address cross-domain few-shot learning, including the ones based on data augmentation, data generation (Wang and Deng, 2021; Yeh et al., 2020; Islam et al., 2021) and self-supervised learning (Phoo and Hariharan, 2020) techniques. However, such data generation and augmentation methods increase the computational cost and cannot scale well to scenarios with higher-shots (Wang and Deng, 2021). Some other works either require large amounts of labeled data from multiple source domains (Hu et al., 2022) or the availability of substantial unlabeled data from the target domain during the source training phase (Phoo and Hariharan, 2020; Islam et al., 2021; Yao, 2021). Such requirements are hard to meet and hence hamper their applicability in many domains. Although some existing prototypical-based few-shot methods have also been applied to address cross-domain few-shot learning due to their simplicity and computational efficiency (Snell et al., 2017; Satorras and Estrach, 2018), these standard methods lack sufficient capacity in handing large domain shifts and adapting to target domains. Moreover, existing methods primarily generate prototypes using metric distances, but often overlook the correla-

Proceedings of the 27th International Conference on Artificial Intelligence and Statistics (AISTATS) 2024, Valencia, Spain. PMLR: Volume 238.

tion between prototypes across categories and struggle with significant cross-domain shifts.

In this paper, we propose a novel Adaptive Parametric Prototype Learning (APPL) method under the meta-learning convention for cross-domain few-shot image classification. APPL introduces a parametric prototype calculator network (PCN) to learn class prototypes from concatenated feature vectors of the support instances. PCN is meta-learned in the source domain. It implements a parametric approach to learn more representative and adaptive prototypes, guided by two tailored loss functions that enhance inter-class discriminability and intra-class cohesion of the prototypes. In the target domain, we deploy a weighted-moving-average (WMA) self-training approach to leverage the unlabeled query instances and fine-tune the prototype-based prediction model in a transductive manner. With PCN and prototype regularizations, the proposed method is expected to have better generalization capacity in learning class prototypes in the feature embedding space, and hence effectively mitigate the domain shift and adapt to the target domain with WMA self-training. Comprehensive experiments are conducted on eight cross-domain few-shot learning benchmark datasets. The empirical results demonstrate the efficacy of the proposed APPL for cross-domain few-shot classification, by comparing with existing state-of-the-art methods.

The contributions of this work are as follows:

1. We propose a novel adaptive prototype learning network called Prototype Calculator Network (PCN). PCN, meta-learned in the source domain, provides a parametric mechanism to generate more informative prototypes with carefully designed prototype regularization loss functions, supporting future adaptation to new target domains.
2. We propose a Weighted-Moving-Average (WMA) self-training strategy for fine-tuning the model in the target domain, tailored specifically for the CDFSL problem. Compared to existing methods, it overcomes the barrier of requiring large amounts of additional data in the target domain and reduces domain shift by generating better pseudo-labels. It enhances the stability and convergence of self-training by jointly employing three mechanisms: Weighted-Moving-Average updating of prediction vectors, a rectified annealing schedule for the WMA, and selectively sampling only the confident pseudo-labels to adapt the model.
3. We conduct extensive experiments. Our proposed method outperforms existing methods on both low-shot (5-shot) and high-shot (20-shot and 50-shot) classification tasks.

2 RELATED WORKS

2.1 Few-Shot Learning

Most FSL studies have focused on the in-domain settings. The FSL approaches can be grouped into three main categories: metric-based and meta-learning approaches (Finn et al., 2017; Snell et al., 2017; Lee et al., 2019), transfer learning approaches (Guo et al., 2019; Jeong and Kim, 2020; Ge and Yu, 2017; Yosinski et al., 2014; Dhillon et al., 2019), and augmentation and generative approaches (Zhang et al., 2018; Lim et al., 2019; Hariharan and Girshick, 2017; Schwartz et al., 2018; Reed et al., 2018). In particular, the representative meta-learning approach, MAML (Finn et al., 2017), learns good initialization parameters from various source tasks that make the model easy to adapt to new tasks. The non-parametric metric-based approach, MatchingNet (Vinyals et al., 2016), employs attention and memory in order to train a network that learns from few labeled samples. ProtoNet (Snell et al., 2017) learns a metric space where each class is represented by the average of the available support instances and classifies query instances based on their distances to the class prototypes. A few meta-learning works, such as RelationNet (Sung et al., 2018), GNN (Satorras and Estrach, 2018) and Transductive Propagation Network (TPN) (Liu et al., 2019), exploit the similarities between support and query instances to classify the query instances. MetaOpt uses meta-learning to train a feature encoder that obtains discriminative features for a linear classifier (Lee et al., 2019). Transfer learning methods initially train a model on base tasks and then use various fine-tuning methods to adapt the model to novel tasks (Guo et al., 2019; Jeong and Kim, 2020; Ge and Yu, 2017; Yosinski et al., 2014; Dhillon et al., 2019). Generative and augmentation approaches generate additional samples to increase the size of available data during training (Zhang et al., 2018; Lim et al., 2019; Hariharan and Girshick, 2017; Schwartz et al., 2018; Reed et al., 2018).

2.2 Cross-Domain Few-shot Learning

Recently cross-domain few-shot learning (CDFSL) has started receiving more attention (Guo et al., 2020; Phoo and Hariharan, 2020). Tseng et al. (2020) propose a feature-wise transformation (FWT) layer that is used jointly with standard few-shot learning methods for cross-domain few-shot learning. The FWT layer uses affine transformations to augment the learned features in order to help the trained network generalize across domains. Du et al. (2022) address the domain shift problem by proposing a prototype-based Hierarchical Variational neural Memory framework (HVM), where the hierarchical prototypes and the memory are

both learned using variational inference. Adler et al. (2023) propose a Cross-domain Hebbian Ensemble Fusion (CHEF) method, which applies an ensemble of Hebbian learners on different layers of the neural network to obtain a representation fusion. Data augmentation and data generation methods have also been used to bridge the gap between the source and target domains (Wang and Deng, 2021; Yeh et al., 2020; Islam et al., 2021). Wang and Deng (2021) propose an Adversarial Task Augmentation approach (ATA) to generate difficult training tasks in an adversarial fashion and improve the generalizability of few-shot methods across largely different domains. Islam et al. (2021) employ dynamic distillation and consistency regularization to train student and teacher networks jointly on the source domain data and unlabeled data from the target domain. Hu et al. (2022) propose domain-switch learning framework with multiple source domains, and use reweighted cross-entropy loss and binary KL divergence loss to prevent overfitting and catastrophic forgetting. Sun et al. (2021) adapt the explanation method of Layer-wise Relevance Propagation (LRP) to the FSL setup, which guides the FSL training by dynamically highlighting the discriminative features of the input samples.

Some other works (Triantafillou et al., 2020; Liu et al., 2021; Bateni et al., 2022; Doersch et al., 2020) have tested alternative cross-domain few-shot learning settings such as Meta-Dataset (Triantafillou et al., 2020) CDFSL setting where models are trained on several source-domain datasets and tested on multiple target-domain datasets. In this work, we focus on the CDFSL setting employed by Guo et al. (2020) as it is the most widely studied cross-domain few-shot learning setting.

3 APPROACH

3.1 Preliminary

The cross-domain few-shot learning problem aims to train a model on the source domain with its large set of labelled instances and then adapt the model to address the prediction task in the target domain with few labeled instances. We assume the two domains have different distributions in the input space ($\mathcal{P}_s \neq \mathcal{P}_t$) and have disjoint classes ($\mathcal{Y}_s \cap \mathcal{Y}_t = \emptyset$). In the target domain, the model is provided with a support set $S = \{(x_i, y_i)\}_{i=1}^{N_s}$ and tested on a query set $Q = \{(x_i, y_i)\}_{i=1}^{N_q}$ where N_s and N_q are the sizes of the support and query sets, respectively. The support set is made up of N classes with K instances in each class, which is commonly described as N-way K-shot.

In the classic prototypical few-shot learning (Snell et al., 2017), each instance x first goes through a feature encoder f_θ to obtain its embedding vector in the feature space. Then, for each class in the support set, a prototype $p_n \in \mathbb{R}^D$ is computed as the average embedding vector of the support instances: $p_n = \frac{1}{K} \sum_{(x,y)\in S_n} f_\theta(x)$, where S_n denotes the set of K support instances from class n. To classify the query instances, the distances between each query sample and the prototypes of all classes in the support set are computed. Then the softmax function is used to normalize the calculated distances to obtain the class prediction probabilities as follows:

$$P(y = j|x) = \frac{\exp(-d(f_\theta(x), p_j))}{\sum_{n=1}^{N} \exp(-d(f_\theta(x), p_n))}, \quad (1)$$

where $d(.,.)$ is a distance function and $P(y = j|x)$ is the predicted probability of query sample x belonging to class j. During the meta-training phase, the model is trained to minimize the cross-entropy loss function as follows:

$$\mathcal{L}_{CE}(Q) = \sum\nolimits_{x\in Q} \ell_{CE}(P_x, Y_x), \quad (2)$$

where ℓ_{CE} is the cross-entropy function, P_x and Y_x are the predicted class probability vector and ground-truth label indicator vector, respectively, for a sample x.

3.2 Adaptive Parametric Prototype Learning

In this section, we present our proposed Adaptive Parametric Prototype Learning (APPL) method for cross-domain few-shot image classification. The overall framework of APPL is illustrated in Figure 1. APPL first performs meta-training in the label-rich source domain by meta learning an adaptive prototype calculator network (PCN) after the feature encoder. PCN generates the prototype of each class by segregating information from the concatenated feature vectors of the K-shot support instances. Then the trained model can be fine-tuned for the few-shot classification task in the target domain using a weighted-moving-average (WMA) self-training approach, which aims to adapt the model to the target domain and further improve the quality of the learned class prototypes. We describe the details below.

3.2.1 Adaptive Prototype Calculator Network

Simply averaging the support instances to calculate the class prototypes has the evident drawback of ignoring the inter-class and intra-class instance relations. To overcome this drawback, we propose to learn class prototypes from the support instances through a parametric prototype calculator network by enforcing both inter-class discriminability and intra-class cohesion in the extracted feature space. Such a parametric prototype generation mechanism is expected to produce

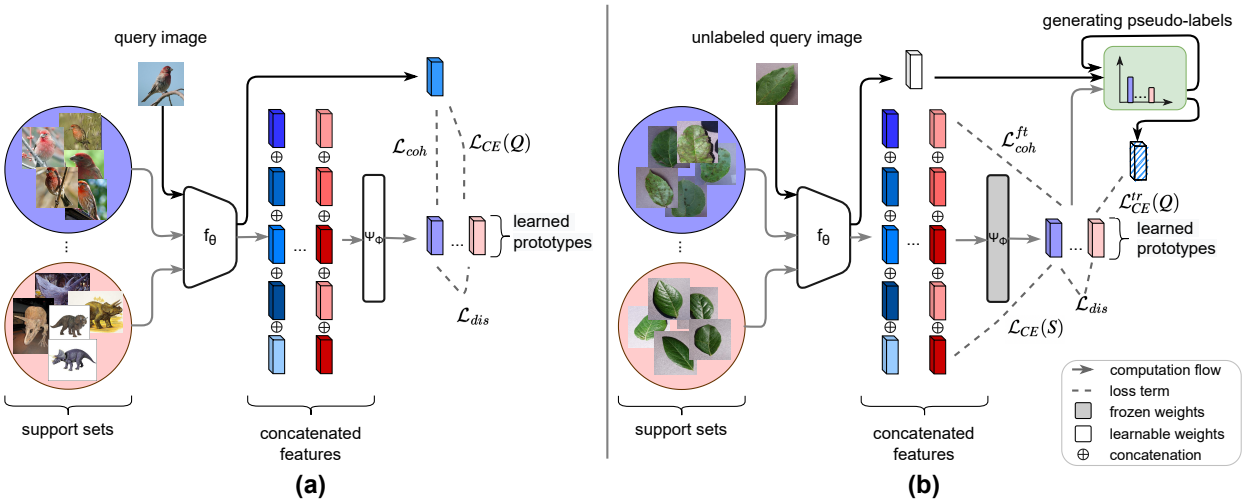

Figure 1: The proposed APPL method. **(a) Training on the source domain**. The concatenated feature vectors of each class are fed into the PCN (ψ_ϕ) to produce class prototypes, which are used to compute the meta-training loss terms on query instances. **(b) Fine-tuning on the target domain.** Both the labelled support set and the unlabeled query set with soft pseudo-labels computed using WMA are used to fine-tune the feature encoder in the target domain with prototype based losses.

more representative class prototypes from various support instance layouts, and guide the feature encoder to better adapt to the target domain through fine-tuning in the testing phase.

We define the adaptive prototype calculator network (PCN) as $\psi_\phi : \mathbb{R}^{K \cdot D} \rightarrow \mathbb{R}^D$, where D is the size of the learned embeddings by the feature encoder, f_θ, K is the number of support instances per class, and ϕ denotes the parameters of the PCN. Specifically, PCN takes the concatenated feature vectors of the support instances of a given class as input, and outputs the prototype of the corresponding class:

$$p_n = \psi_\phi(concat(f_\theta(x_1^n), .., f_\theta(x_K^n))), \tag{3}$$

where x_j^n denotes the j-th support instance from class n and p_n is the learned prototype of class n. By feeding the support instances of each class to ψ_ϕ, we can obtain the prototypes for all the N classes: $\mathbb{P} = \{p_1, p_2, .., p_N\}$.

We train the PCN during the meta-training phase using the few-shot training tasks in the source domain. Specifically, given the feature encoder trained on the support instances, we update the parameters of the PCN by minimizing the cross-entropy loss on the query instances, $\mathcal{L}_{CE}(Q)$. Moreover, we introduce two auxiliary regularization loss terms, a prototype discriminative loss and a prototype cohesive loss, to ensure the learned prototypes are both discriminative and representative of the underlying classes. To elaborate, the prototype discriminative loss $\mathcal{L}_{dis}$ aims to push the prototypes of different classes away from each other and is defined as follows:

$$\mathcal{L}_{dis} = \frac{1}{\sum_{\{p_i, p_j\} \in \mathbb{P}} d(p_i, p_j)}, \tag{4}$$

We in particular use a squared Euclidean distance as $d(\cdot, \cdot)$. By contrast, the prototype cohesive loss $\mathcal{L}_{coh}$ is designed to pull the prototypes and the query instances of their corresponding classes to be closer to each other:

$$\mathcal{L}_{coh} = \sum_{n=1}^{N} \sum_{x \in Q_n} d(p_n, f_\theta(x)), \tag{5}$$

where Q_n denotes the set of query instances from class n. Overall, PCN is meta-trained in the source domain by minimizing the following joint loss:

$$\min_{\phi} \ \mathcal{L}_{train} = \mathcal{L}_{CE}(Q) + \lambda_{dis}\mathcal{L}_{dis} + \lambda_{coh}\mathcal{L}_{coh}, \tag{6}$$

where λ_{dis} and λ_{coh} are the trade-off hyper-parameters that control the contribution of the two regularization loss terms, $\mathcal{L}_{dis}$ and $\mathcal{L}_{coh}$, respectively. The meta-training procedure of our proposed method APPL is summarized in Algorithm 1.

3.2.2 Weighted Moving Average Self-Training

For cross-domain few-shot image classification, significant distribution discrepancies in the input image space typically exist between the source and target domains. Hence after meta-training the feature encoder f_θ and the PCN ψ_ϕ in the source domain, it is critical to fine-tune the feature encoder f_θ on the few-shot test task in the target domain to overcome the cross-domain

Algorithm 1 Training Procedure on Source Domain

Input: Source domain dataset D_s, K, N;
pre-trained feature extractor f_θ;
learning-rate γ_1 and γ_2;
initialize: $\phi \leftarrow \phi_0, \theta \leftarrow \theta_0$;
Output: Learned model parameters θ, ϕ
for iter = 1 **to** maxiters **do**
  $(V, D_s^V) \leftarrow$ randomly sample N class indices from all classes in D_s, and gather their data
  for n in $\{1, .., N\}$ **do**
    $S_n, Q_n \leftarrow$ randomly sample support & query sets for class n from D_s^V
  end for
  $S = S_1 \cup .. \cup S_N, \quad Q = Q_1 \cup .. \cup Q_N$
  for initer=1 **to** maxiniters **do**
    $\theta \leftarrow \theta - \gamma_1 \nabla_\theta \mathcal{L}_{CE}(S)$
  end for
  Compute $\mathcal{L}_{dis}$ and $\mathcal{L}_{coh}$ with Eq. (4) and Eq.(5)
  $\mathcal{L}_{train} = \lambda_{dis}\mathcal{L}_{dis} + \lambda_{coh}\mathcal{L}_{coh}$
  for $(x, y) \in Q$ **do**
    $\mathcal{L}_{train} \leftarrow \mathcal{L}_{train} + \ell_{CE}(x, y)$
  end for
  $\phi \leftarrow \phi - \gamma_2 \nabla_\phi \mathcal{L}_{train}$
end for

gap as well as adapt f_θ to the target test task. Due to the scarcity of the labeled support instances in the target task, we propose to employ the unlabeled query instances with predicted soft pseudo-labels to increase the size and diversity of the target data for fine-tuning and mitigate the domain shift between the source and target domains. To this end, we develop a weighted-moving-average (WMA) self-training approach to compute soft pseudo-labels and deploy the query instances for fine-tuning.

Specifically, at each iteration i of the fine-tuning process, we first calculate the distances between each query instance x and the class prototypes $[p_1^i, p_2^i, \cdots, p_N^i]$ produced by the PCN ψ_ϕ from the support set S for all the N classes, and form the following distance vector for the query instance x:

$$h^i(x) = [d(f_{\theta^i}(x), p_1^i), d(f_{\theta^i}(x), p_2^i), \cdots, d(f_{\theta^i}(x), p_N^i)] \tag{7}$$

Then we use this distance vector $h^i(x)$ to perform weighted moving average update and maintain a weighted-moving-average distance vector $\tilde{h}^i(x)$ for the current iteration i as follows:

$$\tilde{h}^i(x) = \alpha_i \, h^i(x) + (1 - \alpha_i) \, \tilde{h}^{i-1}(x), \tag{8}$$

where α_i is a trade-off parameter that controls the combination weights between distances computed from the current iteration and previous iterations. The weighted-moving-average distance vectors can then be used to

Algorithm 2 Target Domain Fine-tuning Procedure

Input: Target N-way-K-shot test task (S, Q);
source trained model (f_θ, ψ_ϕ);
hyper-parameters λ_{dis}, λ_{coh}, $\alpha_{min}, \alpha_0, \gamma$, ϵ;
initialize: $\theta^1 = \theta$, $\{\tilde{h}^0(x) = 0, \forall x \in Q\}$
Output: Fine-tuned feature encoder parameter θ
for i = 1 **to** maxiters **do**
  $p_n = \psi_\phi(concat(f_\theta(x_1^n), .., f_\theta(x_K^n)))$,
  for $S_n = \{x_1^n, \cdots, x_K^n\}, \forall n \in \{1, \cdots, N\}$
  $\nabla_\theta \mathcal{L}_{ft} \leftarrow 0$
  Compute α_i using Eq.(10)
  for $x \in Q$ **do**
    Compute $\tilde{P}^i(Y|x)$ using Eq.(7)(8)(9).
    $\nabla_\theta \mathcal{L}_{ft} \leftarrow \nabla_\theta \mathcal{L}_{ft} + \nabla_\theta \mathcal{L}_{CE}^{tr}((x, \tilde{P}^i(Y|x)); \theta, \phi)$
  end for
  $\nabla_\theta \mathcal{L}_{ft} \leftarrow \nabla_\theta \mathcal{L}_{ft} + \nabla_\theta \mathcal{L}_{CE}(S) + \lambda_{dis} \nabla_\theta \mathcal{L}_{dis}$
    $+\lambda_{coh} \nabla_\theta \mathcal{L}_{coh}^{ft}$
  $\theta^{i+1} \leftarrow \theta^i - \eta \nabla_{\theta=\theta^i} \mathcal{L}_{ft}$
end for

compute the class prediction probabilities over each query instance x by using the softmax function:

$$\tilde{P}^i(y = j|x) = \frac{\exp(-\tilde{h}_j^i(x))}{\sum_{n=1}^N \exp(-\tilde{h}_n^i(x))}, \tag{9}$$

where $\tilde{P}^i(y = j|x)$ is the probability of the query instance x being assigned to class j at iteration i. By using the predicted class probabilities as soft pseudo-labels, the query instances can subsequently be used to support the fine-tuning of f_θ in a self-training manner. The WMA update mechanism can stabilize the self-training process and dampen possible oscillating predictions for challenging query instances. Moreover, to increase the stability and convergence property of the WMA self-training, we adopt the following rectified annealing schedule for the WMA hyper-parameter α_i:

$$\alpha_i = \gamma \, \alpha_{i-1}, \tag{10}$$

where $\gamma \in (0, 1)$ is a reduction ratio hyper-parameter for updating the α value in each iteration. This annealing schedule can enable larger updates to the $\tilde{h}^i$ vectors in the beginning iterations of fine-tuning by starting with a large value α_0, while gradually reducing the degree of update with the decrease of α_i in later iterations.

With the soft pseudo-labels predicted by the current prototype-based model (θ^i, ϕ), the query instances can be deployed through a cross-entropy loss to guide the further update, i.e., fine-tuning, of the feature encoder f_θ. However, using all pseudo-labeled query instances may lead to noisy updates and negatively impact the model due to the low-confidence predictions of the pseudo-labels. Therefore, we choose to only employ

Table 1: Mean classification accuracy (95% confidence interval in brackets) for 5-way 5-shot classification. * and † denote the results reported in Guo et al. (2020) and Wang and Deng (2021) respectively. Transductive methods are indicated using (T). Methods using Batch Normalization to share query data are denoted with (BN).

	ChestX	CropDisea.	ISIC	EuroSAT	Places	Planate	Cars	CUB
MatchingNet*(Vinyals et al., 2016)	$22.40_{(0.70)}$	$66.39_{(0.78)}$	$36.74_{(0.53)}$	$64.45_{(0.63)}$	–	–	–	–
MAML (BN)*(Finn et al., 2017)	$23.48_{(0.96)}$	$78.05_{(0.68)}$	$40.13_{(0.58)}$	$71.70_{(0.72)}$	–	–	–	–
ProtoNet*(Snell et al., 2017)	$24.05_{(1.01)}$	$79.72_{(0.67)}$	$39.57_{(0.57)}$	$73.29_{(0.71)}$	$58.54_{(0.68)}$	$46.80_{(0.65)}$	$41.74_{(0.72)}$	$55.51_{(0.68)}$
MetaOpt*(Lee et al., 2019)	$22.53_{(0.91)}$	$68.41_{(0.73)}$	$36.28_{(0.50)}$	$64.44_{(0.73)}$	–	–	–	–
RelNet (BN)†(Sung et al., 2018)	$24.07_{(0.20)}$	$72.86_{(0.40)}$	$38.60_{(0.30)}$	$65.56_{(0.40)}$	$64.25_{(0.40)}$	$42.71_{(0.30)}$	$40.46_{(0.40)}$	$56.77_{(0.40)}$
GNN†(Satorras and Estrach, 2018)	$23.87_{(0.20)}$	$83.12_{(0.40)}$	$42.54_{(0.40)}$	$78.69_{(0.40)}$	$70.91_{(0.50)}$	$48.51_{(0.40)}$	$43.70_{(0.40)}$	$62.87_{(0.50)}$
TPN (T)†(Liu et al., 2019)	$22.17_{(0.20)}$	$81.91_{(0.50)}$	$45.66_{(0.30)}$	$77.22_{(0.40)}$	$71.39_{(0.40)}$	$50.96_{(0.40)}$	$44.54_{(0.40)}$	$63.52_{(0.40)}$
MatchingNet+FWT*(Tseng et al., 2020)	$21.26_{(0.31)}$	$62.74_{(0.90)}$	$30.40_{(0.48)}$	$56.04_{(0.65)}$	–	–	–	–
ProtoNet+FWT*(Tseng et al., 2020)	$23.77_{(0.42)}$	$72.72_{(0.70)}$	$38.87_{(0.52)}$	$67.34_{(0.76)}$	–	–	–	–
RelNet+FWT (BN)†(Tseng et al., 2020)	$23.95_{(0.20)}$	$75.78_{(0.40)}$	$38.68_{(0.30)}$	$69.13_{(0.40)}$	$65.55_{(0.40)}$	$44.29_{(0.30)}$	$40.18_{(0.40)}$	$59.77_{(0.40)}$
GNN+FWT†(Tseng et al., 2020)	$24.28_{(0.20)}$	$87.07_{(0.40)}$	$40.87_{(0.40)}$	$78.02_{(0.40)}$	$70.70_{(0.50)}$	$49.66_{(0.40)}$	$46.19_{(0.40)}$	$64.97_{(0.50)}$
TPN+FWT (T) †(Tseng et al., 2020)	$21.22_{(0.10)}$	$70.06_{(0.70)}$	$36.96_{(0.40)}$	$65.69_{(0.50)}$	$66.75_{(0.50)}$	$43.20_{(0.50)}$	$34.03_{(0.40)}$	$58.18_{(0.50)}$
ATA †(Wang and Deng, 2021)	$24.43_{(0.20)}$	$90.59_{(0.30)}$	$45.83_{(0.30)}$	$\mathbf{83.75}_{(0.40)}$	$75.48_{(0.40)}$	$55.08_{(0.40)}$	$49.14_{(0.40)}$	$66.22_{(0.50)}$
LRP-CAN (T) (Sun et al., 2021)	–	–	–	–	$\mathbf{76.90}_{(0.39)}$	$51.63_{(0.41)}$	$42.57_{(0.42)}$	$66.57_{(0.43)}$
LRP-GNN (Sun et al., 2021)	–	–	–	–	$74.45_{(0.47)}$	$54.46_{(0.46)}$	$46.20_{(0.46)}$	$64.44_{(0.48)}$
CHEF(Adler et al., 2023)	$24.72_{(0.14)}$	$86.87_{(0.20)}$	$41.26_{(0.34)}$	$74.15_{(0.27)}$	–	–	–	–
HVM(Du et al., 2022)	$\mathbf{27.15}_{(0.45)}$	$87.65_{(0.35)}$	$42.05_{(0.34)}$	$74.88_{(0.45)}$	–	–	–	–
APPL (T)	$24.87_{(0.41)}$	$\mathbf{92.51}_{(0.84)}$	$\mathbf{46.28}_{(0.64)}$	$79.78_{(0.78)}$	$68.84_{(0.80)}$	$\mathbf{55.20}_{(0.58)}$	$\mathbf{52.67}_{(0.42)}$	$\mathbf{67.46}_{(0.78)}$

query instances with high prediction confidence scores that are larger than a predefined threshold ϵ and compute the query-based cross-entropy loss as follows:

$$\mathcal{L}_{CE}^{tr}(Q) = \sum_{x \in Q} \begin{cases} \mathcal{L}_{CE}(x, \tilde{P}^i(Y|x); \theta, \phi) & \text{if } \max(\tilde{P}^i(Y|x)) > \epsilon \\ 0 & \text{otherwise} \end{cases} \tag{11}$$

where $\tilde{P}^i(Y|x)$ denotes the soft pseudo-label vector computed via Eq.(9) for query instance x, while the maximum predicted probability, $\max(\tilde{P}^i(Y|x))$, is used as the prediction confidence score for x. Here $\mathcal{L}_{CE}(x, \tilde{P}^i(Y|x); \theta, \phi)$ denotes the cross-entropy loss computed over the soft pseudo-labeled pair $(x, \tilde{P}^i(Y|x))$ with f_θ and ψ_ϕ.

In addition to the cross-entropy loss on both the support and query instances, we also use the prototype regularization losses, $\mathcal{L}_{dis}$ and $\mathcal{L}_{coh}$, introduced in the meta-training phase to guide the fine-tuning process. Since the true labels of the query instances are unknown in the meta-testing phase, we modify the prototype cohesive loss $\mathcal{L}_{coh}$ and compute it on the support instances instead:

$$\mathcal{L}_{coh}^{ft} = \sum\nolimits_{n=1}^{N} \sum\nolimits_{x \in S_n} d(p_n, f_\theta(x)), \tag{12}$$

where S_n is the set of support instances from class n. Overall, the feature encoder is fine-tuned by minimizing the following joint loss function with gradient descent:

$$\min_{\theta} \; \mathcal{L}_{ft} = \mathcal{L}_{CE}(S) + \mathcal{L}_{CE}^{tr}(Q) + \lambda_{dis}\mathcal{L}_{dis} + \lambda_{coh}\mathcal{L}_{coh}^{ft} \tag{13}$$

The fine-tuning procedure in the target domain is summarized in Algorithm 2.

3.2.3 Learning with Higher Shots

In order to demonstrate the scalability of the proposed APPL in experimental setups with higher shots, we propose a clustering-based solution to guarantee that the adaptive Prototype Calculator Network scales efficiently with the increase of the number of support samples. By adopting this clustering approach, we ensure that the number of learnable parameters in our proposed PCN is independent of the number of shots, highlighting the scalability of our approach.

Specifically, we first cluster the embeddings of support instances from each class n into K' clusters as follows:

$$\boldsymbol{\mu} = g(f_\theta(x_1^n), \cdots, f_\theta(x_K^n)), \tag{14}$$

where g is the clustering function that takes the learned embeddings of the support instances of a given class as input, and produces the class centroids $\boldsymbol{\mu} = (\mu_1, \mu_2, \cdots, \mu_{K'})$ of the K' clusters. In this process, the clustering function g learns the cluster centroids by minimizing the following loss function:

$$\min_{\boldsymbol{\mu}, c} \mathcal{L}_{clust} = \sum_{j=1}^{K} \sum_{\ell=1}^{K'} \mathbb{1}_{(c_j=\ell)} ||f_\theta(x_j^n) - \mu_\ell||^2, \tag{15}$$

where c is the clustering assignment vector for the K instances. Then, we use the concatenation of the obtained cluster centroid vectors as input to the adaptive PCN as follows:

$$p_n = \psi_\phi(concat(\mu_1, \mu_2, .., \mu_{K'})). \tag{16}$$

Consequently, the number of learnable parameters of our adaptive PCN is unaffected by the number of support instances in each class, which ensures that the

Table 2: Mean classification accuracy (95% confidence interval within brackets) for 5-way 20-shot and 50-shot classification. * denotes results reported in Guo et al. (2020). Transductive methods are indicated using (T). Methods sharing query data via Batch Normalization are indicated using (BN).

	ChestX		CropDiseases		ISIC		EuroSAT	
	20-shot	50-shot	20-shot	50-shot	20-shot	50-shot	20-shot	50-shot
MatchingNet*(Vinyals et al., 2016)	$23.61_{(0.86)}$	$22.12_{(0.88)}$	$76.38_{(0.67)}$	$58.53_{(0.73)}$	$45.72_{(0.53)}$	$54.58_{(0.65)}$	$77.10_{(0.57)}$	$54.44_{(0.67)}$
MAML (BN)*(Finn et al., 2017)	$27.53_{(0.43)}$	–	$89.75_{(0.42)}$	–	$52.36_{(0.57)}$	–	$81.95_{(0.55)}$	–
ProtoNet*(Snell et al., 2017)	$28.21_{(1.15)}$	$29.32_{(1.12)}$	$88.15_{(0.51)}$	$90.81_{(0.43)}$	$49.50_{(0.55)}$	$51.99_{(0.52)}$	$82.27_{(0.57)}$	$80.48_{(0.57)}$
MetaOpt*(Lee et al., 2019)	$25.53_{(1.02)}$	$29.35_{(0.99)}$	$82.89_{(0.54)}$	$91.76_{(0.38)}$	$49.42_{(0.60)}$	$54.80_{(0.54)}$	$79.19_{(0.62)}$	$83.62_{(0.58)}$
RelNet (BN)*(Sung et al., 2018)	$26.63_{(0.92)}$	$28.45_{(1.20)}$	$80.45_{(0.64)}$	$85.08_{(0.53)}$	$41.77_{(0.49)}$	$49.32_{(0.51)}$	$74.43_{(0.66)}$	$74.91_{(0.58)}$
MatchingNet+FWT*(Tseng et al., 2020)	$23.23_{(0.37)}$	$23.01_{(0.34)}$	$74.90_{(0.71)}$	$75.68_{(0.78)}$	$32.01_{(0.48)}$	$33.17_{(0.43)}$	$63.38_{(0.69)}$	$62.75_{(0.76)}$
ProtoNet+FWT*(Tseng et al., 2020)	$26.87_{(0.43)}$	$30.12_{(0.46)}$	$85.82_{(0.51)}$	$87.17_{(0.50)}$	$43.78_{(0.47)}$	$49.84_{(0.51)}$	$75.74_{(0.70)}$	$78.64_{(0.57)}$
RelNet+FWT(BN)*(Tseng et al., 2020)	$26.75_{(0.41)}$	$27.56_{(0.40)}$	$78.43_{(0.59)}$	$81.14_{(0.56)}$	$43.31_{(0.51)}$	$46.38_{(0.53)}$	$69.40_{(0.64)}$	$73.84_{(0.60)}$
CHEF(Adler et al., 2023)	$29.71_{(0.27)}$	$31.25_{(0.20)}$	$94.78_{(0.12)}$	$96.77_{(0.08)}$	$54.30_{(0.34)}$	$60.86_{(0.18)}$	$83.31_{(0.14)}$	$86.55_{(0.15)}$
HVM(Du et al., 2022)	$30.54_{(0.47)}$	$32.76_{(0.46)}$	$95.13_{(0.35)}$	$97.83_{(0.33)}$	$54.97_{(0.35)}$	$61.71_{(0.32)}$	$84.81_{(0.34)}$	$87.16_{(0.35)}$
APPL (T)	$\mathbf{30.75}_{(0.41)}$	$\mathbf{33.14}_{(0.88)}$	$\mathbf{95.77}_{(0.53)}$	$\mathbf{98.14}_{(0.56)}$	$\mathbf{57.97}_{(0.73)}$	$\mathbf{62.17}_{(0.43)}$	$\mathbf{88.60}_{(0.85)}$	$\mathbf{89.75}_{(0.76)}$

proposed APPL is scalable and easy to apply in scenarios with a higher number of shots.

4 EXPERIMENTS

4.1 Experimental Setup

Datasets We conducted comprehensive experiments on eight cross-domain few-shot learning (CDFSL) benchmark datasets. We use MiniImageNet (Vinyals et al., 2016) as the single source domain dataset, and use the following eight datasets as the target domain datasets: CropDiseases (Mohanty et al., 2016), EuroSAT (Helber et al., 2019), ISIC (Tschandl et al., 2018), ChestX (Wang et al., 2017), CUB (Wah et al., 2011), Cars (Krause et al., 2013), Places (Zhou et al., 2017) and Planate (Van Horn et al., 2018). We use the same train/val/test split as that used by Guo et al. (2020). We select the hyperparameters based on the model accuracy on the MiniImageNet validation set.

Implementation Details We use ResNet10 (He et al., 2016) as our backbone network and use a simple network made up of a single linear layer followed by ReLU activation to represent PCN. We train our prototype-based prediction model (feature encoder and PCN) on the source domain for 400 epochs with 100 meta-training tasks and 15 query instances per class. Adam optimizer with a weight decay of 1e-2 and a learning rate of 1e-6 is used to train the APPL. The trade-off parameters λ_{dis} and λ_{coh} are set to 0.1 and 1e-3 respectively. The proposed APPL is evaluated on 600 randomly selected few-shot learning tasks in each target domain. We fine-tune the feature encoder for 100 iterations for each task with a learning rate of 1e-2. The fine-tuning hyperparameters, α_0, γ, and ϵ, take the values of 0.5, 0.99, and 0.4, respectively.

4.2 Comparison Results

4.2.1 Learning with Few Shots

We first evaluate the performance of the proposed APPL method on the common cross-domain 5-way 5-shot classification tasks. We compare APPL with both a set of representative FSL methods (MatchingNet (Vinyals et al., 2016), MAML (Finn et al., 2017), ProtoNet (Snell et al., 2017), RelationNet (Sung et al., 2018), MetaOpt (Lee et al., 2019), GNN (Satorras and Estrach, 2018) and TPN (Liu et al., 2019)) and five state-of-the-art CDFSL methods (FWT (Tseng et al., 2020), ATA (Wang and Deng, 2021), LRP (Sun et al., 2021), CHEF (Adler et al., 2023) and HVM (Du et al., 2022)). FWT has been applied jointly with five standard FSL methods: MatchingNet, ProtoNet, RelationNet, GNN and TPN. LRP has been applied jointly with two standard FSL methods: GNN and Cross-attention network (CAN). The comparison results are presented in Table 1, where the top part of the table reports the results of the standard FSL methods and the bottom part reports the CDFSL results.

We can see that the CDFSL methods (ATA, CHEF, HVM, LRP and APPL) designed specifically to handle vast differences between source and target domains perform largely better than the standard FSL works developed for in-domain settings. FWT however only produces improvements in most cases over its base RelationNet. Notably, the proposed APPL outperforms all standard FSL methods including ProtoNet and ProtoNet+FWT on all the eight datasets. In particular, its performance gain over ProtoNet is remarkable, exceeding 10% on four out of the eight datasets, which highlights the importance of the PCN. In addition, APPL outperforms all the CDFSL methods on five datasets, and produces the second best results on two datasets. These results demonstrate the effectiveness of the proposed APPL method for CDFSL.

Table 3: Ablation study results in terms of mean classification accuracy (95% confidence interval within brackets) for cross-domain 5-way 5-shot classification tasks.

	ChestX	CropDisea.	ISIC	EuroSAT	Places	Planate	Cars	CUB
ProtoNet	$24.05_{(1.01)}$	$79.72_{(0.67)}$	$39.57_{(0.57)}$	$73.29_{(0.71)}$	$58.54_{(0.68)}$	$46.80_{(0.65)}$	$41.74_{(0.72)}$	$55.51_{(0.68)}$
APPL	$\mathbf{24.87}_{(0.41)}$	$\mathbf{92.51}_{(0.84)}$	$\mathbf{46.28}_{(0.64)}$	$\mathbf{79.78}_{(0.78)}$	$\mathbf{68.84}_{(0.80)}$	$55.20_{(0.58)}$	$\mathbf{51.67}_{(0.42)}$	$\mathbf{67.46}_{(0.78)}$
−w/o ψ_ϕ	$22.33_{(0.56)}$	$89.11_{(0.66)}$	$43.99_{(0.68)}$	$77.99_{(0.68)}$	$67.57_{(0.33)}$	$53.69_{(0.60)}$	$50.30_{(0.81)}$	$64.03_{(0.97)}$
−w/o $\mathcal{L}_{dis}$	$24.84_{(0.69)}$	$91.31_{(0.72)}$	$43.23_{(0.82)}$	$78.25_{(0.76)}$	$66.18_{(0.49)}$	$54.56_{(0.84)}$	$51.56_{(0.85)}$	$60.45_{(0.85)}$
−w/o $\mathcal{L}_{coh}$	$23.77_{(0.68)}$	$90.19_{(0.76)}$	$43.69_{(0.49)}$	$79.53_{(0.71)}$	$65.89_{(0.47)}$	$51.62_{(0.77)}$	$50.32_{(0.81)}$	$60.96_{(0.85)}$
−w/o $\mathcal{L}_{CE}(S)$	$21.08_{(0.42)}$	$59.15_{(0.59)}$	$26.90_{(0.78)}$	$49.95_{(0.80)}$	$34.79_{(0.85)}$	$25.72_{(0.77)}$	$27.19_{(0.87)}$	$30.12_{(0.74)}$
−w/o $\mathcal{L}^{tr}_{CE}(Q)$	$22.36_{(0.42)}$	$88.24_{(0.86)}$	$42.14_{(0.59)}$	$77.63_{(0.65)}$	$67.14_{(0.82)}$	$\mathbf{55.69}_{(0.60)}$	$51.59_{(0.82)}$	$60.22_{(0.85)}$
−w/o WMA	$21.15_{(0.45)}$	$90.12_{(0.87)}$	$44.95_{(0.62)}$	$77.12_{(0.67)}$	$67.68_{(0.83)}$	$54.76_{(0.62)}$	$49.94_{(0.85)}$	$65.87_{(0.87)}$

4.2.2 Learning with Higher Shots

We further investigated CDFSL with higher-shot tasks in the target domain. In particular, we evaluate APPL with cross-domain 5-way 20-shot and 5-way 50-shot learning tasks on 4 target-domain datasets (ChestX, CropDiseases, ISIC and EuroSAT). To handle higher-shot problems and increase the scalability of APPL, we extend APPL by adding a clustering function g prior to the PCN component. As discussed previously, this clustering approach ensures that the number of learnable parameters of our proposed PCN is independent of the number of shots, preserving the scalability of our proposed approach. Specifically, we use the g function to cluster the support instances in each class into $K' = 5$ clusters based on their learned embeddings. The obtained cluster centroid vectors are then concatenated as input for PCN. We compared APPL with both standard FSL methods and several CDFSL methods, and the results are presented in Table 2.

As observed from the results, the methods designed for CDFSL (CHEF, HVM, and APPL) continue to demonstrate superior performance compared to the standard FSL methods. The performance gains of APPL over ProtoNet and ProtoNet+FWT are remarkable, exceeding 6% and 9% on three datasets (CropDiseases, ISIC and EuroSAT) in the cases of 20-shot and 50-shot, respectively. Moreover, the APPL method consistently achieved the best results across all four datasets, outperforming both the traditional FSL methods and the other CDFSL methods for the 20-shot and 50-shot cases. These results again validate the effectiveness of APPL for CDFSL and demonstrate its capacity to handle cross-domain higher-shot learning problems. Two factors account for our proposed method's good performance in the case of higher shots: First, benefiting from the proposed WMA self-training strategy in the target domain, we are able to generate more accurate pseudo-labels with higher shots, which enables our model to obtain better results. Second, we conduct clustering over the embeddings of support instances to generate class centroids with higher shots, which can eliminate some noisy information and allow the PCN to learn more representative features.

4.3 Ablation Study

To investigate the importance of each component of our APPL approach, we conducted an ablation study to compare APPL with its six variants: (1) "−w/o ψ_ϕ", which drops PCN and replaces it with a simple average of the support instances of each class. (2) "−w/o $\mathcal{L}_{dis}$", which drops the $\mathcal{L}_{dis}$ loss. (3) "−w/o $\mathcal{L}_{coh}$", which drop the $\mathcal{L}_{coh}$ loss. (4) "−w/o $\mathcal{L}_{CE}(S)$", which drops the cross-entropy loss over the support instances in fine-tuning. (5) "−w/o $\mathcal{L}^{tr}_{CE}(Q)$", which drops the cross-entropy loss over the query instances and hence discards the WMA self-training component in fine-tuning. (6) "−w/o WMA", which drops the weighted moving average when determining the pseudo-labels, and instead leverages the predictions generated by the model from the previous iteration as the pseudo-labels. In addition, we also compared with "ProtoNet", which can be considered as a baseline variant of APPL that drops PCN, WMA self-training, $\mathcal{L}_{dis}$ and $\mathcal{L}_{coh}$.

We compared APPL with these variants in the cross-domain 5-way 5-shot setting on all the eight datasets, and the results are reported in Table 3. We can see that APPL outperforms all the variants on almost all datasets. The "−w/o $\mathcal{L}_{CE}(S)$" variant produced the largest performance drop among all variants, which highlights the importance of the few labeled support instances for fine-tuning in the target domain. The performance degradation for ProtoNet and "−w/o ψ_ϕ" highlights the importance of the proposed PCN component. In addition, "−w/o ψ_ϕ" outperforms ProtoNet, which underlines the performance gain obtained by using pseudo-labeled query instances with WMA self-training and the prototype regularization losses in the absence of PCN. The other four variants, "−w/o $\mathcal{L}_{dis}$", "−w/o $\mathcal{L}_{coh}$", "−w/o $\mathcal{L}^{tr}_{CE}(Q)$", and "−w/o WMA" also perform worse than APPL, which verifies the contributions of the two prototype regularization loss terms and the WMA self-training component respectively.

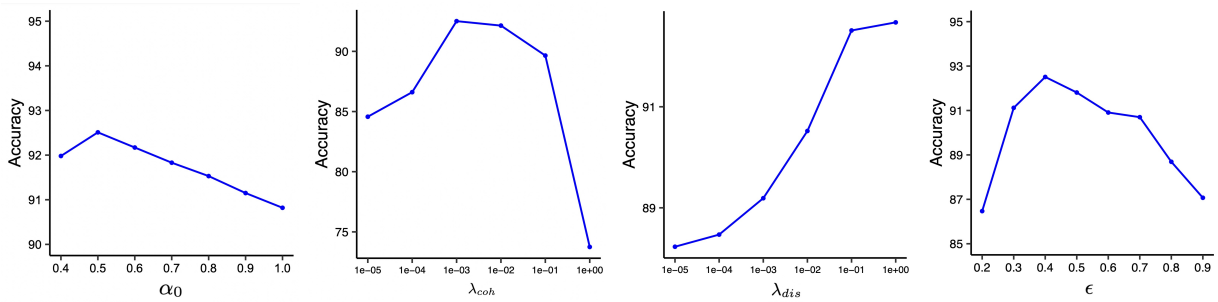

Figure 2: Sensitivity analysis over hyperparameters α_0, λ_{coh}, λ_{dis}, and ϵ on the CropDisease dataset with cross-domain 5-way 5-shot tasks.

Table 4: Impact of the input order for the Adaptive Prototype Calculator Network (PCN). The results are mean classification accuracies (95% confidence interval within brackets) on 5-way 5-shot classification tasks.

	ChestX	CropDisea.	ISIC	EuroSAT
Perm # 1	$24.79_{(0.36)}$	$92.37_{(0.77)}$	$46.12_{(0.55)}$	$79.69_{(0.72)}$
Perm # 2	$24.68_{(0.35)}$	$92.73_{(0.78)}$	$46.29_{(0.54)}$	$79.57_{(0.72)}$
Perm # 3	$24.82_{(0.36)}$	$92.52_{(0.77)}$	$46.28_{(0.56)}$	$79.68_{(0.74)}$
Perm # 4	$24.90_{(0.36)}$	$92.54_{(0.76)}$	$46.18_{(0.55)}$	$79.79_{(0.74)}$
Perm # 5	$24.87_{(0.41)}$	$92.51_{(0.84)}$	$46.28_{(0.64)}$	$79.78_{(0.78)}$

4.4 Impact of the Input Order

Since the concatenated embeddings of the support set instances are fed as input to the adaptive PCN to generate the prototype of each class, it is important to validate the impact of this concatenation order on the performance of APPL. Therefore, after fine-tuning, we evaluate the performance of APPL with different concatenation orders of the support instances using the cross-domain 5-way 5-shot learning tasks on 4 different datasets. We generate 5 different random permutations of the input support samples and report the corresponding results for each permutation in Table 4. We can see the results are very similar across different permutation orders, which validates the resilience of PCN to the concatenation order of the input instances.

4.5 Hyperparameter Analysis

We investigated the impact of four hyperparameters $(\alpha_0, \lambda_{coh}, \lambda_{dis}, \epsilon)$ on the performance of APPL, and summarize the results in Figure 2. Each plot in Figure 2 presents the results of APPL with different values for the corresponding hyperparameter on the CropDisease dataset under the cross-domain 5-way 5-shot task. From the results we can see that APPL is not very sensitive to the choice of value for α_0, as the performance change of APPL across all values of α_0 is relatively very small. As for λ_{coh}, a large value or an excessively small value will influence the query/support instances to be pulled more strongly or weakly towards the class prototypes, consequently negatively impacting the results. A reasonable λ_{coh} value between 1e-1 and 5e-3 is required to obtain reasonable performance. In the case of λ_{dis}, the experimental results improve as the value of λ_{dis} increases, and the results become stable when the parameter reaches 1e-1. We believe this is due to that λ_{dis} controls the contribution of the $\mathcal{L}_{dis}$ loss that pushes the prototypes of different classes away from each other; when the distances between the prototypes are larger than a certain threshold, general instance embeddings are no longer susceptible to mutual influence for making predictions. Finally, it is worth noting that ϵ is an important hyperparameter, which controls the confident level of the pseudo-labels selected for fine-tuning in the target domain. When ϵ is too small, more unlabeled query samples are used in fine-tuning with their noisy pseudo-labels, and when ϵ is too large, very few unlabeled query samples can be used in fine-tuning. Both situations can negatively impact the performance of the approach. Experimental results show that when a moderate value of 0.4 is selected for ϵ, the number and accuracy of the selected pseudo-labels can be well balanced, achieving the best result.

5 CONCLUSION

In this paper, we proposed a novel Adaptive Parametric Prototype Learning (APPL) method to address the cross-domain few-shot learning problem. APPL meta-trains an adaptive prototype calculator network in the source domain to learn more discriminative and representative class prototypes which can then guide the feature encoder to adapt to the target domain through fine-tuning. Moreover, a WMA self-training strategy is adopted to enhance fine-tuning by exploiting the unlabeled query instances in the target domain to mitigate domain shift and avoid overfitting to support instances. Experiment results show that APPL surpasses state-of-the-art methods on eight cross-domain few-shot classification benchmarks.

References

Adler, T., Brandstetter, J., Widrich, M., Mayr, A., Kreil, D., et al. (2023). Cross-domain few-shot learning by representation fusion. *Scientific Reports*.

Bateni, P., Barber, J., van de Meent, J.-W., and Wood, F. (2022). Enhancing few-shot visual classification with unlabelled examples. In *Proceedings of the IEEE/CVF Winter Conference on Applications of Computer Vision*.

Dhillon, G. S., Chaudhari, P., Ravichandran, A., and Soatto, S. (2019). A baseline for few-shot image classification. In *International Conference on Learning Representations (ICLR)*.

Doersch, C., Gupta, A., and Zisserman, A. (2020). Crosstransformers: spatially-aware few-shot transfer. In *Advances in Neural Information Processing Systems (NeurIPS)*.

Du, Y., Zhen, X., Shao, L., and Snoek, C. G. M. (2022). Hierarchical variational memory for few-shot learning across domains. In *International Conference on Learning Representations (ICLR)*.

Finn, C., Abbeel, P., and Levine, S. (2017). Model-agnostic meta-learning for fast adaptation of deep networks. In *International conference on machine learning (ICML)*.

Ge, W. and Yu, Y. (2017). Borrowing treasures from the wealthy: Deep transfer learning through selective joint fine-tuning. In *Proceedings of the IEEE conference on computer vision and pattern recognition (CVPR)*.

Guo, Y., Codella, N. C., Karlinsky, L., Codella, J. V., Smith, et al. (2020). A broader study of cross-domain few-shot learning. In *European Conference on Computer Vision (ECCV)*.

Guo, Y., Shi, H., Kumar, A., Grauman, K., Rosing, T., and Feris, R. (2019). Spottune: transfer learning through adaptive fine-tuning. In *Proceedings of the IEEE/CVF conference on computer vision and pattern recognition (CVPR)*.

Hariharan, B. and Girshick, R. (2017). Low-shot visual recognition by shrinking and hallucinating features. In *Proceedings of the IEEE International Conference on Computer Vision (ICCV)*.

He, K., Zhang, X., Ren, S., and Sun, J. (2016). Deep residual learning for image recognition. In *Proceedings of the IEEE conference on computer vision and pattern recognition (CVPR)*.

Helber, P., Bischke, B., Dengel, A., and Borth, D. (2019). Eurosat: A novel dataset and deep learning benchmark for land use and land cover classification. *IEEE Journal of Selected Topics in Applied Earth Observations and Remote Sensing*.

Hu, Z., Sun, Y., and Yang, Y. (2022). Switch to generalize: Domain-switch learning for cross-domain few-shot classification. In *International Conference on Learning Representations (ICLR)*.

Islam, A., Chen, C.-F. R., Panda, R., Karlinsky, L., Feris, R., and Radke, R. J. (2021). Dynamic distillation network for cross-domain few-shot recognition with unlabeled data. In *Advances in Neural Information Processing Systems (NeurIPS)*.

Jeong, T. and Kim, H. (2020). Ood-maml: Meta-learning for few-shot out-of-distribution detection and classification. In *Advances in Neural Information Processing Systems (NeurIPS)*.

Krause, J., Stark, M., Deng, J., and Fei-Fei, L. (2013). 3D object representations for fine-grained categorization. In *Proceedings of the IEEE international conference on computer vision workshops*.

Lee, K., Maji, S., Ravichandran, A., and Soatto, S. (2019). Meta-learning with differentiable convex optimization. In *Proceedings of the IEEE/CVF Conference on Computer Vision and Pattern Recognition (CVPR)*.

Lim, S., Kim, I., Kim, T., Kim, C., and Kim, S. (2019). Fast autoaugment. In *Advances in Neural Information Processing Systems (NeurIPS)*.

Liu, Y., Lee, J., Park, M., Kim, S., Yang, E., Hwang, S., and Yang, Y. (2019). Learning to propagate labels: Transductive propagation network for few-shot learning. In *International Conference on Learning Representations (ICLR)*.

Liu, Y., Lee, J., Zhu, L., Chen, L., Shi, H., and Yang, Y. (2021). A multi-mode modulator for multi-domain few-shot classification. In *Proceedings of the IEEE/CVF International Conference on Computer Vision (ICCV)*.

Mohanty, S. P., Hughes, D. P., and Salathé, M. (2016). Using deep learning for image-based plant disease detection. *Frontiers in plant science*.

Phoo, C. P. and Hariharan, B. (2020). Self-training for few-shot transfer across extreme task differences. In *International Conference on Learning Representations (ICLR)*.

Reed, S., Chen, Y., Paine, T., van den Oord, A., Eslami, S. A., Rezende, D., Vinyals, O., and de Freitas, N. (2018). Few-shot autoregressive density estimation: Towards learning to learn distributions. In *International Conference on Learning Representations (ICLR)*.

Satorras, V. G. and Estrach, J. B. (2018). Few-shot learning with graph neural networks. In *International Conference on Learning Representations (ICLR)*.

Schwartz, E., Karlinsky, L., Shtok, J., Harary, S., Marder, et al. (2018). Delta-encoder: an effective sample synthesis method for few-shot object recognition. In *Advances in Neural Information Processing Systems (NeurIPS)*.

Snell, J., Swersky, K., and Zemel, R. (2017). Prototypical networks for few-shot learning. In *Advances in neural information processing systems (NeurIPS)*.

Sun, J., Lapuschkin, S., Samek, W., Zhao, Y., Cheung, N.-M., and Binder, A. (2021). Explanation-guided training for cross-domain few-shot classification. In *2020 25th International Conference on Pattern Recognition (ICPR)*.

Sung, F., Yang, Y., Zhang, L., Xiang, T., Torr, P. H., and Hospedales, T. M. (2018). Learning to compare: Relation network for few-shot learning. In *Proceedings of the IEEE conference on computer vision and pattern recognition (CVPR)*.

Triantafillou, E., Zhu, T., Dumoulin, V., Lamblin, et al. (2020). Meta-dataset: A dataset of datasets for learning to learn from few examples. In *International Conference on Learning Representations (ICLR)*.

Tschandl, P., Rosendahl, C., and Kittler, H. (2018). The ham10000 dataset, a large collection of multi-source dermatoscopic images of common pigmented skin lesions. *Scientific data*.

Tseng, H.-Y., Lee, H.-Y., Huang, J.-B., and Yang, M.-H. (2020). Cross-domain few-shot classification via learned feature-wise transformation. In *International Conference on Learning Representations (ICLR)*.

Van Horn, G., Mac Aodha, O., Song, Y., Cui, Y., Sun, et al. (2018). The inaturalist species classification and detection dataset. In *Proceedings of the IEEE conference on computer vision and pattern recognition (CVPR)*.

Vinyals, O., Blundell, C., Lillicrap, T., Wierstra, D., et al. (2016). Matching networks for one shot learning. In *Advances in neural information processing systems (NeurIPS)*.

Wah, C., Branson, S., Welinder, P., Perona, P., and Belongie, S. (2011). The caltech-ucsd birds-200-2011 dataset. California Institute of Technology.

Wang, H. and Deng, Z.-H. (2021). Cross-domain few-shot classification via adversarial task augmentation. In *International Joint Conferences on Artificial Intelligence (IJCAI)*.

Wang, X., Peng, Y., Lu, L., Lu, Z., Bagheri, M., and Summers, R. M. (2017). Chestx-ray8: Hospital-scale chest x-ray database and benchmarks on weakly-supervised classification and localization of common thorax diseases. In *Proceedings of the IEEE conference on computer vision and pattern recognition (CVPR)*.

Yao, F. (2021). Cross-domain few-shot learning with unlabelled data. *arXiv preprint arXiv:2101.07899*.

Yeh, J.-F., Lee, H.-Y., Tsai, B.-C., Chen, Y.-R., Huang, P.-C., and Hsu, W. H. (2020). Large margin mechanism and pseudo query set on cross-domain few-shot learning. *arXiv preprint arXiv:2005.09218*.

Yosinski, J., Clune, J., Bengio, Y., and Lipson, H. (2014). How transferable are features in deep neural networks? In *Advances in neural information processing systems (NeurIPS)*.

Zhang, R., Che, T., Ghahramani, Z., Bengio, Y., and Song, Y. (2018). Metagan: An adversarial approach to few-shot learning. In *Advances in neural information processing systems (NeurIPS)*.

Zhou, B., Lapedriza, A., Khosla, A., Oliva, A., and Torralba, A. (2017). Places: A 10 million image database for scene recognition. *IEEE transactions on pattern analysis and machine intelligence (TPAMI)*.

Checklist

1. For all models and algorithms presented, check if you include:
   (a) A clear description of the mathematical setting, assumptions, algorithm, and/or model. [Yes]
   (b) An analysis of the properties and complexity (time, space, sample size) of any algorithm. [No]
   (c) (Optional) Anonymized source code, with specification of all dependencies, including external libraries. [No]

2. For any theoretical claim, check if you include:
   (a) Statements of the full set of assumptions of all theoretical results. [Not Applicable]
   (b) Complete proofs of all theoretical results. [Not Applicable]
   (c) Clear explanations of any assumptions. [Not Applicable]

3. For all figures and tables that present empirical results, check if you include:
   (a) The code, data, and instructions needed to reproduce the main experimental results (either in the supplemental material or as a URL). [No]
   (b) All the training details (e.g., data splits, hyperparameters, how they were chosen). [Yes]
   (c) A clear definition of the specific measure or statistics and error bars (e.g., with respect to the random seed after running experiments multiple times). [Yes]
   (d) A description of the computing infrastructure used. (e.g., type of GPUs, internal cluster, or cloud provider). [No]

4. If you are using existing assets (e.g., code, data, models) or curating/releasing new assets, check if you include:
   (a) Citations of the creator If your work uses existing assets. [Yes]
   (b) The license information of the assets, if applicable. [Not Applicable]
   (c) New assets either in the supplemental material or as a URL, if applicable. [Not Applicable]
   (d) Information about consent from data providers/curators. [Not Applicable]
   (e) Discussion of sensible content if applicable, e.g., personally identifiable information or offensive content. [Not Applicable]

5. If you used crowdsourcing or conducted research with human subjects, check if you include:
   (a) The full text of instructions given to participants and screenshots. [Not Applicable]
   (b) Descriptions of potential participant risks, with links to Institutional Review Board (IRB) approvals if applicable. [Not Applicable]
   (c) The estimated hourly wage paid to participants and the total amount spent on participant compensation. [Not Applicable]